

Differential Cellular Expression of Isoforms of Inositol 1,4,5-Triphosphate Receptors in Neurons and Glia in Brain

ALAN H. SHARP,^{1,2,3*} FREDERICK C. NUCIFORA, JR.,^{2,3} OLIVIER BLONDEL,⁴ CAROL A. SHEPPARD,⁵ CHUANYI ZHANG,^{1,3} SOLOMON H. SNYDER,^{3,6,7} JAMES T. RUSSELL,⁵ DAVID K. RYUGO,^{6,8} AND CHRISTOPHER A. ROSS^{2,3,6}

¹Laboratory of Cellular Neurobiology, Johns Hopkins University School of Medicine, Baltimore, Maryland 21287

²Laboratory of Molecular Neurobiology, Johns Hopkins University School of Medicine, Baltimore, Maryland 21205

³Department of Psychiatry, Johns Hopkins University School of Medicine, Baltimore, Maryland 21287

⁴Laboratory of Molecular Biology, NINDS, NIH, Bethesda, Maryland 20892

⁵Laboratory of Cellular and Molecular Neurophysiology, NICCHD, NIH, Bethesda, Maryland 20892

⁶Department of Neuroscience, Johns Hopkins University School of Medicine, Baltimore, Maryland 21205

⁷Department of Pharmacology and Molecular Sciences, Johns Hopkins University School of Medicine, Baltimore, Maryland 21205

⁸Department of Otolaryngology/Head and Neck Surgery, Johns Hopkins University School of Medicine, Baltimore, Maryland 21205

ABSTRACT

Inositol 1,4,5-trisphosphate receptors (IP₃R) are mediators of second messenger-induced intracellular calcium release. Three isoforms are known to be expressed in brain, but their regional distributions and cellular localizations are little known. In order to better understand the roles of IP₃ receptor isoforms in brain function, a first step is to define their distributions. We have used affinity-purified antibodies directed against peptides unique to each isoform to determine their sites of expression in rat brain. Type 1 IP₃R (IP₃R1) is dramatically enriched in Purkinje neurons in cerebellum and neurons in other regions, consistent with previous studies. By contrast, IP₃R2 is only detected in glia, whereas IP₃R3 is predominantly neuronal, with little detected in glia. IP₃R3 is enriched in neuropil, especially in neuronal terminals (which often contain large dense core vesicles) in limbic and basal forebrain regions including olfactory tubercle, central nucleus of the amygdala, and bed nucleus of the stria terminalis. In addition, IP₃R1 and IP₃R3 have clearly distinct time courses of expression in developing brains. These data suggest separate roles for inositol 1,4,5-trisphosphate receptor isoforms in development, and for glial and neuronal function. The IP₃R3 may be involved in regulation of neurotransmitter or neuropeptide release in terminals within specific nuclei of the basal forebrain and limbic system. *J. Comp. Neurol.* 406:207-220, 1999. © 1999 Wiley-Liss, Inc.

Indexing terms: Ca²⁺ release; electron microscopy; synapse; second messengers; neuropeptides; limbic system

Intracellular calcium is an important messenger molecule in neurons and other cells (Ross et al., 1990; Berridge, 1993; Bootman and Berridge, 1995; Clapham, 1995; De Camilli et al., 1996; Striggow and Ehrlich, 1996). Intracellular calcium signaling is especially important in the brain and is believed to be involved in long-term

Grant sponsor: NIH; Grant numbers: MH43040 and DC-00232; Grant sponsor: USSPHS; Grant number: MH18501; Grant sponsor: Research Scientist Award; Grant number: DA-00074; Grant sponsor: National Research Council.

*Correspondence to: Alan H. Sharp, Meyer Building, Rm 2-181, Johns Hopkins Univ. School of Med., 600 N. Wolfe St., Baltimore, MD 21287. E-mail: ahsharp@welchlink.welch.jhu.edu

Received 8 May 1998; Revised 6 October 1998; Accepted 26 October 1998

modulation of neuronal excitability and plasticity (Berridge, 1993; Simpson et al., 1995). One source of intracellular calcium is release from intracellular stores via the second messenger inositol trisphosphate (IP₃; Ferris and Snyder, 1992; Berridge, 1993; Furuichi and Mikoshiba, 1995; Striggow and Ehrlich, 1996). Hormone, neurotransmitter, or growth factor stimulation of cell surface receptors leads to the generation of IP₃ and gating of calcium from these stores via IP₃ receptors (IP₃R).

The IP₃R has been purified from rat cerebellum (Supatapone et al., 1988) and localized primarily to the endoplasmic reticulum (ER; Mignery et al., 1989; Ross et al., 1989) though nuclear, plasma membrane and neurotransmitter vesicle localizations have also been described (Khan et al., 1992; Furuichi et al., 1994; Furuichi and Mikoshiba, 1995; Petersen, 1996). Molecular cloning reveals three different isoforms encoded by different genes, IP₃R1, 2, and 3 (Furuichi et al., 1989; Mignery et al., 1989; Sudhof et al., 1991; Ross et al., 1992; Blondel et al., 1993; Maranto, 1994; De Smedt et al., 1997). Regulation of IP₃ receptors is complex with alternative splicing of at least IP₃R1 (Mignery et al., 1990; Nakagawa et al., 1991; Danoff et al., 1991; Schell et al., 1993; Nucifora et al., 1995) and post-translational modification of IP₃R by phosphorylation (Danoff et al., 1991; Ferris et al., 1991; Furuichi et al., 1994). In addition, there is regulation by adenine nucleotides (Ferris et al., 1990), calcium (Finch et al., 1991; Bezprozvanny et al., 1991; Iino and Endo, 1992), and the immunophilin FK506 binding protein (FKBP-12; Cameron et al., 1995). Different isoforms of the receptor may have different affinities for IP₃ and different forms of regulation (Sudhof et al., 1991; Blondel et al., 1993; Maranto, 1994; Newton et al., 1994; Sugiyama et al., 1994a,b; Joseph et al., 1995; Wojcikiewicz, 1995; DeLisle et al., 1996). Receptors in a number of cell lines appear to be heterotetramers composed of more than one isoform (Joseph et al., 1995; Monkawa et al., 1995; Wojcikiewicz and He, 1995; Nucifora et al., 1996), and there is evidence for homotetramers of the IP₃R3 isoform in some cultured cells (Nucifora et al., 1996) with the possibility that homotetramers of other isoforms could also exist. Among tissues, only liver has so far been demonstrated to contain IP₃R heterotetramers (Monkawa et al., 1995).

The separate isoforms of IP₃Rs have different tissue distributions, with IP₃R1 being most highly expressed in brain, IP₃R2 apparently being highly expressed in spinal cord, and IP₃R3 highly expressed in intestine (Ross et al., 1992; Maranto, 1994; Newton et al., 1994). Different isoforms also predominate in different culture cell types (Blondel et al., 1993; De Smedt et al., 1994; Sugiyama et al., 1994a,b; Parys et al., 1995; Nucifora et al., 1996).

Within the brain, the distribution of radiolabeled IP₃ binding and IP₃R immunoreactivity has been described (Worley et al., 1989; Otsu et al., 1990; Satoh et al., 1990; Sharp et al., 1993a,b; Ryugo et al., 1995), but most studies did not distinguish among IP₃R isoforms. The distribution of IP₃R1 mRNA throughout the brain has been described by using *in situ* hybridization (Mailleux et al., 1992; Furuichi et al., 1993), and two studies have examined the distribution of IP₃R1 receptor protein in the brain by using isoform-specific antibodies (Nakanishi et al., 1991; Dent et al., 1996). IP₃R1 is expressed at high levels in cerebellar Purkinje cells and at lower levels in other regions. Although IP₃R1 is the most abundant isoform in the brain, other isoforms are present (Sudhof et al., 1991; Ross et al.,

1992; Blondel et al., 1993). A study of IP₃ binding in brains of mice homozygous for IP₃R1 gene deletions detected residual IP₃ binding in most regions of brain (Matsumoto et al., 1996), implying widespread distribution of other receptor isoforms. One study reported the presence of IP₃R3 in glia in rat brain (Yamamoto-Hino et al., 1995), but used an antibody raised against a peptide differing significantly from the rat sequence and has not been confirmed. Besides regional and cellular variations, IP₃R isoforms may differ in neuronal compartmentalization. IP₃R1 occurs in dendrites, dendritic spines, cell bodies, axons, and axonal terminals of cerebellar Purkinje cells, but appears to be more compartmentalized in most other neurons with highest levels generally in cell bodies and proximal dendrites (Nakanishi et al., 1991; Ryugo et al., 1995; Dent et al., 1996). Little is known of the intracellular compartmentalization of other isoforms in the brain.

We have now examined the expression of the relatively uncharacterized IP₃R2 and IP₃R3 isoforms in rat brains by Western blot and immunohistochemistry, including experiments on the well-characterized IP₃R1 for comparison. We have found that IP₃R1 and IP₃R3 have differing time courses of expression in development and have demonstrated differing localizations of IP₃Rs 1, 2, and 3 in populations of neurons and glia in adult brains. In contrast to a previous study of IP₃R3 in the brain (Yamamoto-Hino et al., 1995), we detect IP₃R3 predominately in neuronal structures, especially neuronal terminals, and we describe, for the first time, the distribution of IP₃R2 in the brain.

MATERIALS AND METHODS

Animals

All work involving animals was approved by the animal care and use committees of the institutions where the work was performed and was in accordance with NIH guidelines.

Preparation of antibodies

Antisera were raised in rabbits (Cocalico Biologicals, Reamstown, PA) against synthetic peptides corresponding to unique portions of IP₃R1, 2, and 3 as described previously (Nucifora et al., 1995). Three peptides GHPHNMN-VNPQQPA, GSNTPHENHHMPPH, and RRQLGFVDVQNCMSR, corresponded to the C-termini of IP₃R1, 2, and 3, respectively, whereas a fourth peptide, VSEVSVEI-LEED, corresponded to a unique internal portion (amino acids 2432–2444) of IP₃R3. Antibodies were affinity-purified by using the peptide immunogen immobilized on a solid support as previously described (Nucifora et al., 1995). Affinity-purified antibodies specific for IP₃R1, 2, and 3 C-termini were prepared from the sera of rabbits 41, 42, and 75 and were respectively termed AP41, AP42, and AP75. Affinity-purified antibodies specific for the internal type 3 IP₃R peptide were prepared from the serum of rabbit 45 and were termed AP45.

Because the C-terminal IP₃R3 peptide used to generate antibodies (AP75) was not freely soluble at pH 7.4, another peptide corresponding to this region was synthesized (DDLGLFVDVQNCMSR) with three aspartates added in place of the N-terminal RRQR to increase solubility. This peptide eliminated immunoreactivity in preadsorption controls with antibody AP75.

Western blot analysis

For characterization of antibodies and analysis of protein distribution by immunoblot, 6- to 8-week-old Sprague-Dawley white rats (Harlan, Indianapolis, IN) were decapitated and the brains removed, dissected, and homogenized in ice-cold buffer (50 mM Tris-HCl [pH 7.4], 1 mM EDTA, 1 mM 2-mercaptoethanol, 0.4 mM phenylmethylsulfonyl fluoride [PMSF], 1 mM benzamidine, 1 µg/ml leupeptin, 0.5 µg/ml antipain, 1 µg/ml aprotinin, 1 µg/ml chymostatin, 1 µg/ml pepstatin A) using a Brinkmann Polytron (Brinkmann, Westbury, NY). Protein was assayed with the Coomassie Plus reagent (Pierce, Rockford, IL). For developmental studies, timed pregnant female Sprague-Dawley white rats were decapitated and embryos harvested. Tissues were homogenized and protein assayed as above. Primary cultures of rat cortical astrocytes were prepared and harvested as described below. Protein (200 µg per lane) was subjected to electrophoresis on sodium dodecylsulfate (SDS)-polyacrylamide gels (3–12% gradients). Prestained molecular weight standards (Gibco-BRL, Gaithersburg, MD) were run in adjacent lanes. Apparent molecular masses are reported as indicated by the manufacturer. Proteins were transferred electrophoretically to nitrocellulose membranes. Blots were preincubated for 1 hour at room temperature in 5% nonfat dry milk in phosphate-buffered saline (PBS, pH 7.4) before incubation overnight at 4°C with antibody diluted in 3% bovine serum albumin (BSA) in PBS. AP41 was used at 1–2 µg/ml, AP42 was used at 2 µg/ml, and AP75 was used at 3 µg/ml. For preblockade controls, antibodies were preincubated overnight at 4°C with the appropriate peptide immunogens (10 µg/ml). After incubation in antibody, blots were washed for 15 minutes in 5% nonfat dry milk in PBS, followed by three more washes of 5 minutes each in the same solution. Blots were then incubated with secondary antibodies (peroxidase-linked, affinity-purified goat anti-rabbit from Boehringer-Mannheim, Indianapolis, IN) at a dilution of 1:10,000 for 1 hour at room temperature. After three washes (1 × 15 minutes and 2 × 5 minutes) in 5% nonfat dry milk in PBS, the blots were washed two times more in PBS. Blots were then developed by using the Lumi Glo chemiluminescence reagents (Kirkegaard and Perry, Gaithersburg, MD). Images of Western blots (Figs. 1 and 2) were digitized by using a flat-bed scanner, adjusted slightly by using brightness and contrast controls (Adobe Photoshop 3.0), labeled with text and printed in a high-resolution format with a color printer (Fuji Pictography 3000).

Primary culture of rat cortical astrocytes

Cultures were prepared from 2-day-old rats according to methods previously described (McCarthy and de Vellis, 1980). Briefly, cells were grown in plastic flasks until reaching confluence (9 days in culture). The flasks were placed on an orbital shaker and vigorously agitated for 3 hours to remove microglia, and the medium was discarded and replaced with fresh medium. The flasks were then shaken vigorously overnight. The type 1 astrocytes, which remain firmly attached to the culture flasks, were harvested as follows. Culture plates were rinsed three times with ice-cold PBS. Cells were then scraped into cold PBS, pelleted by centrifugation, resuspended in a small volume of cold homogenization buffer with protease inhibitors (50 mM Tris-HCl [pH 7.4], 1 mM EDTA, 1 mM 2-mercaptoethanol, 0.4 mM PMSF, 1 mM benzamidine, 1 µg/ml leupep-

tin, 0.5 µg/ml antipain, 1 µg/ml aprotinin, 1 µg/ml chymostatin, 1 µg/ml pepstatin A) and homogenized with several brief bursts from a probe sonicator. Soluble and particulate fractions were prepared by centrifugation of the homogenates at 100,000 × g for 1 hour at 4°C. Protein was assayed by using the Coomassie Plus reagent (Pierce). Alternatively, cells were rinsed three times with cold PBS and then scraped on ice into a small volume of 50 mM Tris-HCl (pH 7.4), 5% SDS, 10 mM benzamidine, 0.8 mM PMSF. In this case, protein was assayed using the BCA reagent (Pierce).

Immunohistochemistry

Light microscopy. Immunoperoxidase localization in rat brain sections. Rats (6- to 8-week-old, Sprague-Dawley white; Harlan) were deeply anesthetized with pentobarbital (130 mg/kg) and perfused with 25–50 ml of PBS followed by 200–300 ml of 4% paraformaldehyde in 100 mM sodium phosphate (pH 7.3). Tissue was then removed and further fixed by immersion in the same fixative solution for 2–4 hours at 4°C. Tissue was then cryoprotected by overnight incubation in 20% glycerol in PBS. After freezing the tissue under powdered dry ice, sections (40-µm-thick) were cut into PBS with a sliding microtome. Some sections were stored at -20°C in an antifreeze solution (10% [w/v] polyvinylpyrrolidone [PVP-40], 30% [w/v] sucrose, 10% [w/v] ethylene glycol, and 50 mM sodium phosphate [pH 7.4]). Before staining, sections were rinsed in 50 mM Tris, (pH 7.4), 1.5% NaCl (TBS), and permeabilized by incubation in 0.3% Triton X-100 in TBS for 20–30 minutes at room temperature with gentle agitation. Sections were then blocked by incubation in 5% normal goat serum (NGS) in TBS for 30 minutes at room temperature. Affinity-purified antibodies were diluted in 1% NGS in TBS. AP41 (IP₃R1) was used at a concentration of 1–2 µg/ml, AP42 (IP₃R2) was used at 0.5–2 µg/ml, and AP75 (IP₃R3) was used at 3 µg/ml. For preadsorption controls, diluted antibodies were preincubated overnight with 10 µg/ml of the appropriate peptide immunogen at 4°C before use. Sections were incubated with antibody solutions overnight at 4°C with gentle agitation, washed three times for 10 minutes each, and then processed with the Vectastain Elite avidin/biotinylated peroxidase reagents (Vector Labs, Burlingame, CA) as follows. Sections were incubated 1 hour with biotinylated goat anti-rabbit secondary antibody (1:200) in 1% NGS in TBS at room temperature, washed 10 minutes in 1% NGS in TBS, followed by three washes of 7 minutes each in TBS alone and then incubated with avidin-biotinyl peroxidase complex (1:50 dilution of each reagent in TBS) for 1 hour at room temperature. After washing three times for 10 minutes each, sections were developed using 0.5 µg/ml diaminobenzidine (DAB) and 0.1% H₂O₂ in TBS. Sections were rinsed, mounted on glass slides, dehydrated in graded ethanol solutions, cleared with xylene, and coverslipped. Anatomical localizations were determined by comparison of stained sections with the rat brain atlas of Paxinos and Watson (1986) and by consultation with other experts in rat brain anatomy (see ACKNOWLEDGMENTS).

Immunoperoxidase localization of IP₃R3 in COS-7 cells. A full-length cDNA clone, pCMV-IP₃R3, was prepared and inserted into the *EcoRI* site of the expression vector pCMV6b (Blondel et al., 1993). COS-7 (African green monkey fibroblast) cells were transfected with pCMV-IP₃R3 and pCMV6b DNA by electroporation (GenePulse,

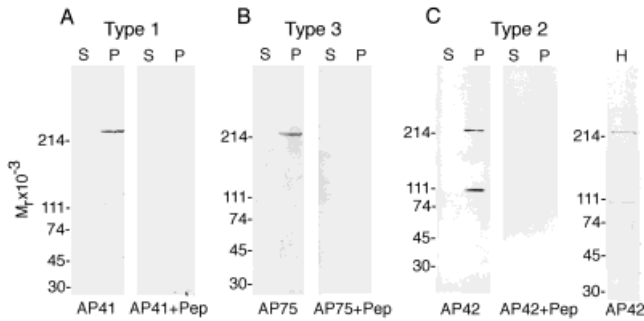


Fig. 1. Western blot characterization of isoform-specific anti-inositol 1,4,5-trisphosphate receptors (IP₃R) antibodies. Soluble (S) and particulate (P) fractions were prepared from rat olfactory bulb tissue (A and B) and cultured cortical astrocytes (C), and proteins (200 µg per lane) were resolved on 3–12% sodium dodecylsulfate (SDS) polyacrylamide gels and transferred to nitrocellulose membranes. The blots were stained with affinity-purified antibodies against IP₃R1 (A, AP41), IP₃R3 (B, AP75), and IP₃R2 (C, AP42). A single band of approximately 260-kDa in the particulate fractions was stained by each of the IP₃R1- and IP₃R3-specific antibodies (A, AP41 and B, AP75, respectively). In addition to a band of approximately 260 kDa, another band of approximately 100 kDa was labeled with the IP₃R2-specific antibody (C, AP42). All immunoreactivity was eliminated by preincubation of the antibodies with 10 µg/ml of the corresponding peptide immunogens (blots labeled +Pep). The 100-kDa band labeled by the IP₃R2-specific antibody varied in intensity among preparations and was nearly absent in a crude homogenate prepared by scraping the cells directly into a solution containing 5% SDS, 50 mM Tris-HCl (pH 7.4), 10 mM benzamide, and 0.8 mM PMSF (H), suggesting that this band is a proteolytic fragment of the IP₃R2.

Bio-Rad, Hercules, CA). Expression of IP₃R activity was measured after 65 hours by ligand binding and immunoblotting. Transfected cells were cultured for 65 hours on glass coverslips and then fixed with 4% paraformaldehyde. Cells were stained for IP₃R3 with antibody AP75 as described for sections.

Immunofluorescent colocalization of IP₃R2 and S100-β in brain sections. Rats were deeply anesthetized with pentobarbital (as indicated above) and perfused with 4% paraformaldehyde plus 0.1% glutaraldehyde in phosphate buffer. Brains were removed, postfixed in 4% paraformaldehyde for 2–4 hours, cryoprotected, sectioned on a sliding microtome (35-µm-thick), and stored in antifreeze solution at -20°C until use. Sections were then washed in PBS, permeabilized and blocked as for immunoperoxidase labeling and then incubated overnight at 4°C in the absence (control) or presence of antibody AP42. After four washes in PBS, sections were incubated for 1.5 hours in anti-S100-β monoclonal antibody (1:10,000; Sigma, St. Louis, MO) and washed again. The sections were then incubated with the appropriate fluorescent secondary antibodies (fluorescein isothiocyanate [FITC]-labeled goat anti-mouse and/or indocarbocyanine [Cy3]-labeled goat anti-rabbit, Jackson Immunoresearch, West Grove, PA), washed in PBS, mounted on glass slides, and coverslipped with a buffered medium containing Mowiol (Calbiochem, San Diego, CA) and glycerol with DABCO (1,4 diazabicyclo-[2.2.2]octane; Sigma) added as an anti-fade agent (Osborn and Weber, 1982).

Sections were imaged with a fluorescence microscope equipped with a cooled charge coupled device digital camera as described previously (Sheppard et al., 1997). Images were processed with a digital confocal restoration

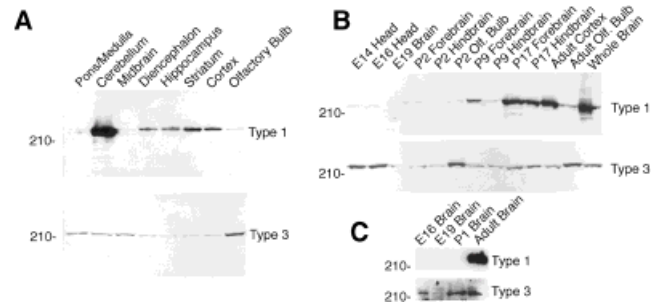


Fig. 2. Western blot analysis of inositol 1,4,5-trisphosphate receptors (IP₃R)1 and IP₃R3 expression in adult (A) and developing (B and C) rat brains. Crude membranes were prepared from adult rat brain regions (A) and analyzed by Western blot. Lanes each contained 200 µg protein. In adult brain, expression of the IP₃R1 was highest in cerebellum, low in pons/medulla, midbrain and olfactory bulb, and at intermediate levels in the striatum, cortex, hippocampus, and diencephalon, whereas IP₃R3 was more evenly distributed with enrichment in the olfactory bulb. Western blot analysis of homogenates prepared from rat head or brain at various stages in development (B and C) showed that IP₃R1 and IP₃R3 had strikingly different patterns of expression during development. IP₃R1 increased relatively late in development, whereas IP₃R3 was detected at earlier times. The blots in C were stained with different aliquots of antibody and were exposed to film somewhat longer than those in B. E, embryonic day; P, postnatal day.

algorithm developed by Dr. Frederick Fay and colleagues at the University of Massachusetts (Carrington et al., 1992; Carter et al., 1993) as described previously (Sheppard et al., 1997). This algorithm was implemented by using the software system Cell Scan (CSPI-Scanalytics Inc., Billerica, MA). Cellscan, the integrated software/hardware system (CSPI-Scanalytics, Billerica, MA) controlled both the CCD camera and a piezoelectric microscope fine focus controller such that optical sections of specimens (0.25 µm) could be obtained. We first characterized blurring due to the optics by measuring the point-spread function of the imaging system by acquiring a series of optical sections of a latex bead filled with the same fluorophore (diameter = 0.2 µm). Sections were imaged under identical conditions and routinely 53 optical sections were obtained 0.25 µm apart. The Cellscan software was then utilized to computationally reverse the blurring resulting from out-of-focus plane light. The protocol was experimentally tested using the fluorescent beads that were previously used for acquiring the point-spread function of the microscope. The axial resolution of our microscope under these measurement conditions was 0.75 µm. Restored images were displayed as reconstructed volume views. Omission of anti-IP₃R2 (AP42) gave no signal in the red channel, indicating specificity of label and lack of bleed-through of green label into the red channel. Similarly, red label did not bleed into the green channel. Images of S100-β and IP₃R2 staining (Fig. 6) were pseudo-colored green and red, respectively. The images were imported into Adobe Photoshop 5.0 and merged to test for colocalization (yellow). Images were then printed in CMYK color to a dye sublimation printer (Tektronix Phaser) or displayed in RGB color on a high-resolution monitor.

Electron microscopy. Rats were deeply anesthetized and then perfused with freshly prepared 4% paraformaldehyde in 120 mM sodium cacodylate buffer (pH 7.4) with 0.008% CaCl₂ at 37°C. A few other rats were perfused with

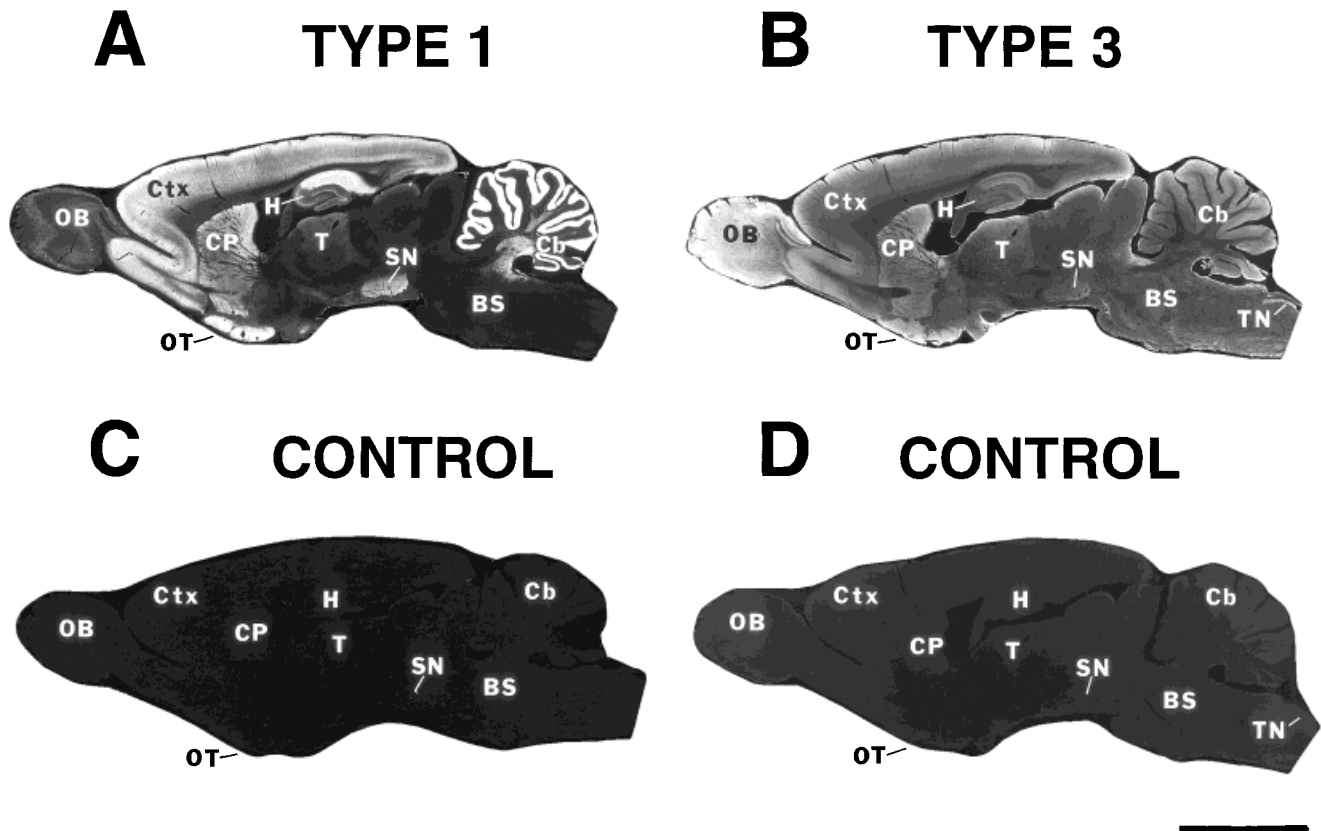


Fig. 3. Immunohistochemical distribution of IP₃R1 (A) and IP₃R3 (B) in sagittal rat brain sections. Sections taken within 80 μ m of each other were stained with antibodies specific for IP₃R1 (AP41) (A) or IP₃R3 (AP75) (B) using an indirect immunoperoxidase method. In these dark field views dense label appears bright against a dark background. Immunoreactivity was abolished by preincubation of the

antibodies with the appropriate peptide immunogen (C and D). BS, brainstem; Cb, cerebellum; Ctx, cerebral cortex; CP, caudate putamen; H, hippocampus; OB, olfactory bulb; OT, olfactory tubercle; T, thalamus; SN, substantia nigra; TN, caudal spinal trigeminal nucleus. Scale bar = 5 mm.

a buffered solution containing 4% paraformaldehyde and 2% acrolein. Brains were removed and postfixed for 2–4 hours in the perfusion fixative. Sections were then cut at 50- μ m thickness with a Vibratome and processed for immunoperoxidase staining as above with the omission of the Triton X-100 permeabilization step. Adjacent or nearly identical control sections were identically processed with antigen-adsorbed antibody as above. Immunostained and control sections were rinsed in TBS, washed six times for 5 minutes each in a solution containing 120 mM sodium phosphate (pH 7.4), 8% dextrose, and 0.008% CaCl₂ and then placed in 1% osmium tetroxide for 15 minutes. The sections were then washed five times for 10 minutes each in 100 mM maleate buffer (pH 5.2), stained en block in 1% uranyl acetate overnight at 4°C, and washed again. The sections were dehydrated in increasing concentrations of ethanol, infiltrated with Epon and flat-embedded between two sheets of Aclar (Ted Pella, Inc., Redding, PA). Relevant parts of sections were identified under a light microscope, dissected out, and reembedded in BEEM capsules for sectioning. Ultrathin sections were collected onto Formvar-coated slotted grids, stained with 7% uranyl acetate, and examined with a JEOL 100CX electron microscope. Methods have been previously described in more detail (Ryugo et al., 1991). Electron microscopy negatives were scanned and digitized (Leafscan 45), optimized by using only

brightness and contrast features (Adobe Photoshop 3.0), and printed in high-resolution format with a color printer (Fuji Pictography 3000).

RESULTS

Isoform-specific antisera were generated against synthetic peptides corresponding to the unique C-terminal portions of IP₃R1, 2, and 3 and specific antibodies were affinity-purified. Their characterization and use in endocrine cell lines for Western blots and immunofluorescence have been described (Nucifora et al., 1996). To determine the specificity of the antibodies in brain tissue, we performed Western blots on soluble and particulate fractions prepared from rat brain homogenates. Both affinity-purified anti-IP₃R1 (AP 41) and IP₃R3 (AP 75) antibodies labeled single bands in the particulate fractions (Fig. 1A and B, lanes P) but no bands in the soluble fractions (Fig. 1A and B, lanes S) with IP₃R1 running at about 260 kDa and IP₃R3 slightly smaller. These results are consistent with the known properties of the IP₃R1 and 3 (Supattapone et al., 1988; Furuichi et al., 1989; Sudhof et al., 1991; Blondel et al., 1993; Joseph et al., 1995; Wojcikiewicz, 1995). Western blots on membranes from various regions of rat brain did not yield any specific signal with the anti-IP₃R2. However, because immunohistochemistry

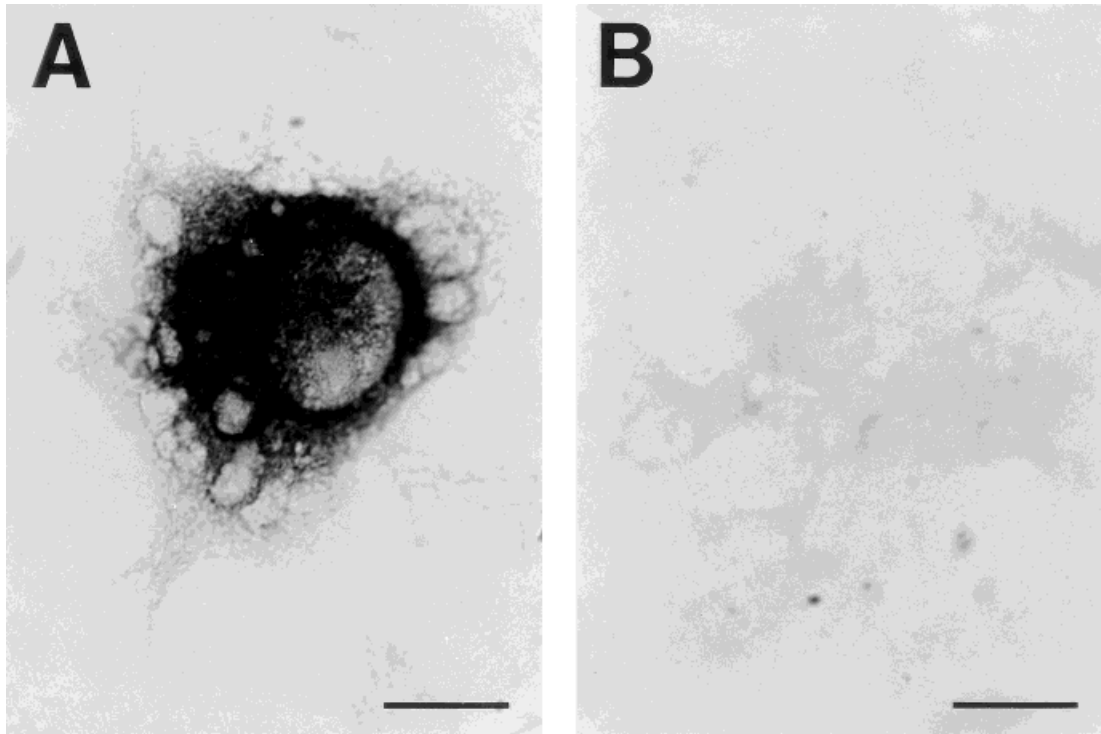


Fig. 4. Immunohistochemical detection of IP₃R3 in transfected COS cells. To more closely examine the suitability of IP₃R3-specific antibody (AP75) for immunohistochemistry, COS-7 cells transfected with pCMV-IP₃R3 were fixed with 4% paraformaldehyde (the same fixative used for brain sections) and stained for IP₃R3 using the

immunoperoxidase method. Transfected cells stained intensely with type 3-specific antibody (AP75) (A) and immunoreactivity was blocked by preincubation with the peptide immunogen (B), indicating that AP75 can specifically recognize IP₃R3 under these conditions. Scale bars = 20 μ m.

showed enrichment of IP₃R2 in glial cells (see below), we performed Western blot analysis of soluble and particulate fractions prepared from primary cultures of type 1 astroglial cells. In this preparation, the anti-IP₃R2 yielded a band in the particulate fraction running slightly smaller than IP₃R1, but stained no bands in the soluble fraction (Fig. 1C, lane S). In addition, the anti-IP₃R2 detected a prominent band at around 100 kDa in the particulate fraction (Fig. 1C, lane P). This band varied in intensity in different preparations and was almost eliminated in a homogenate prepared by rapidly harvesting the cells directly into denaturing buffer containing SDS (Fig. 1C, lane H). These results suggest that the 100-kDa band is due to proteolytic breakdown of the receptors, consistent with previous evidence that proteolysis of IP₃R during homogenization gives rise to a fragment of this size (Mourey et al., 1989). Immunoreactivity of each antibody was eliminated by preincubation of the antibody with the peptide immunogen indicating specificity (Fig. 1, +PEP). In addition, incubation of the antibodies with the peptides for the other receptors did not alter reactivity (Nucifora et al., 1996; and data not shown). Together, these data suggest that the affinity-purified antibodies AP41, AP42, and AP75 can specifically detect IP₃R1, 2 and 3, respectively.

We compared regional distributions of IP₃R1 and IP₃R3 by Western blot analysis (Fig. 2A). IP₃R1 localizations fit well with previous reports of very high densities in the cerebellum and low densities in the olfactory bulb (Nakanishi et al., 1991; Dent et al., 1996). By contrast, IP₃R3 was enriched in the olfactory bulb. IP₃R1 levels varied greatly

in different brain regions, whereas IP₃R3 levels were more uniform throughout the brain.

IP₃R3 and IP₃R1 also differed markedly in expression during development. On Western blots (lanes loaded for equal protein), IP₃R1 levels were low but just detectable at embryonic day (E)14, E16, and postnatal day (P)2, began to increase in P9 forebrain and, by P17, attained adult levels in forebrain and hindbrain (Fig. 2B). By contrast, the substantial IP₃R3 levels in E14 and E16 heads were at least as high as in adult brain. Levels appeared lower in E19 brain but thereafter increased, although not nearly as sharply as IP₃R1. In the olfactory bulb, IP₃R3 already attained adult levels at P2.

In a separate experiment, brains were isolated from embryos and assayed by Western blot for IP₃R1 and 3 (Fig. 2C). IP₃R1 levels appeared undetectable in E16, E19, and P1 brains (Fig. 2C), although a very long exposure revealed faint bands at all three points (not shown). By contrast, IP₃R3 was readily detectable in E16 brain. The level appeared lower in E19 brain and by P1 was similar to that of adult whole brain samples. The IP₃R3 level in E16 brain (Fig. 2C) appeared lower, relative to adult brain, than in a whole head sample (Fig. 2B), suggesting that there is significant expression in the embryo head outside the brain. The data in Figure 2 show that IP₃R1 and 3 expressions are clearly distinctly regulated according to brain region and developmental period.

Immunohistochemical mapping in adult brain confirmed and extended the Western blot analysis (Fig. 3). In much of the brain, IP₃R1 distribution (Fig. 3A) grossly

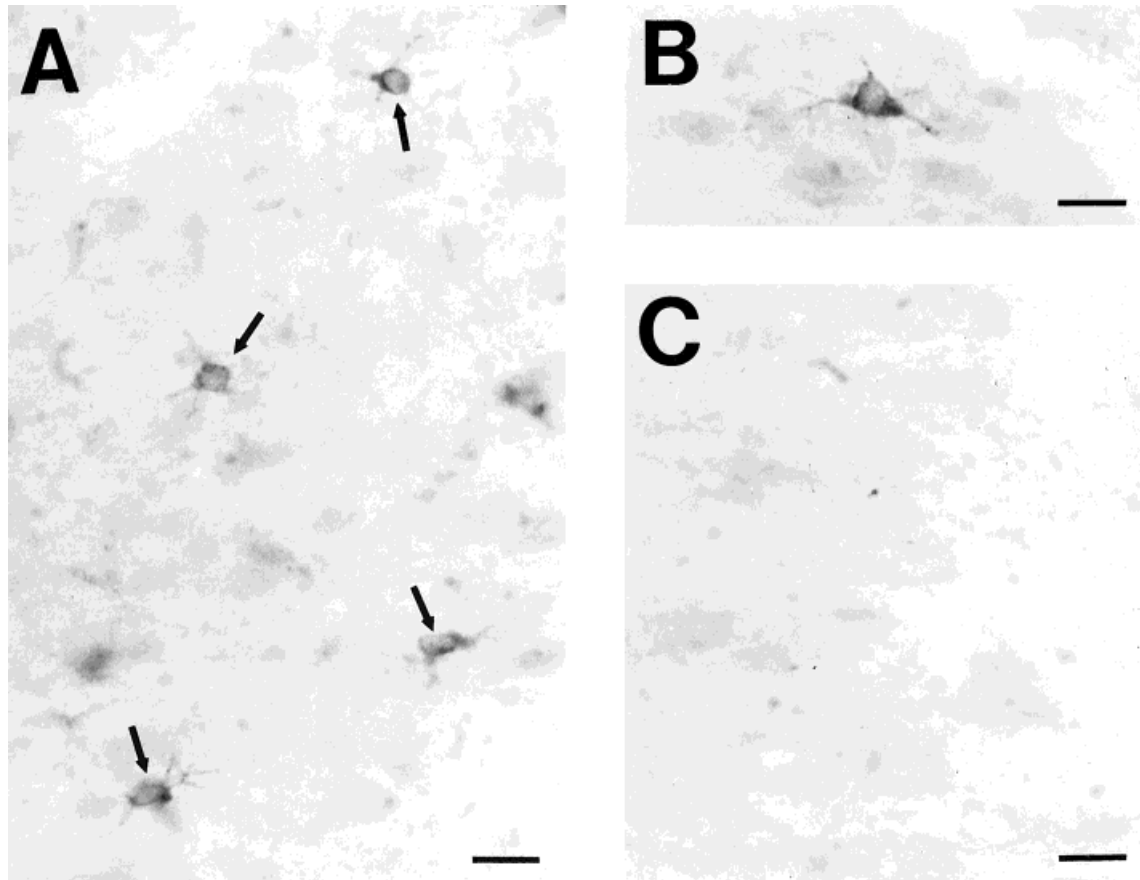


Fig. 5. Localization of IP₃R2 in rat brain sections. Specific immunoperoxidase label for IP₃R2 (using antibody AP42) appeared only in scattered small cells resembling glia (A, examples indicated by arrows, and B). Staining was abolished when antibodies were preincubated with the peptide immunogen (C). Scale bar = 20 μ m.

resembled autoradiographic localizations of [³H]IP₃ binding (Worley et al., 1989; Matsumoto et al., 1996), reflecting the relative abundance of this isoform in many parts of the brain. ([³H]IP₃ binding was not previously examined in the olfactory bulb). The distribution was also in general agreement with previous studies using IP₃R1-specific antibodies (Nakanishi et al., 1991; Dent et al., 1996). By contrast, the distribution of IP₃R3 by immunohistochemistry (Fig. 3B) was quite different, with relatively high levels in the olfactory bulb and tubercle, and modest labeling in the cerebellar cortex, the cerebral cortex, the hippocampus, the caudate-putamen, the amygdala, and regions of the basal forebrain. This distribution corresponds well to that seen in the Western blot experiments (Fig. 2A). Staining for both isoforms of the receptor was abolished when the antibodies were pretreated with the appropriate peptide immunogen (Fig. 3C and D).

Because our results on IP₃R3 distribution differed significantly from a previously published report (Yamamoto-Hino et al., 1995; see DISCUSSION), we sought to confirm the specificity of the anti-IP₃R3 for immunohistochemistry on formaldehyde-fixed tissue. Accordingly, we stained COS-7 cells, transfected with the cDNA for IP₃R3, after preserving with the same fixative and using the same immunoperoxidase method as used for tissue sections (Fig. 4). In this experiment, approximately 1% of the cells were strongly

labeled, corresponding well with the transfection efficiency of approximately 1% in this experiment (data not shown). The label appeared to be distributed similarly to the pattern of endoplasmic reticulum (Fig. 4A) as previously reported for COS-7 cells transfected with the IP₃R3 cDNA (Blondel et al., 1993). When AP75 was preincubated with the peptide immunogen (Fig. 4B) or omitted (not shown), no cells were labeled. Staining with the other antibody to IP₃R3 (AP45) gave a pattern generally similar to that of AP75 (data not shown). Thus, anti-IP₃R3 antibody AP75 can specifically detect IP₃R3 in formaldehyde-fixed material.

The antibodies against IP₃R2 (AP42) labeled only scattered cells in brain sections as seen with the aid of a light microscope (Fig. 5A and B). These cells had multiple small processes and morphology consistent with that of glial cells. Specific label in other cell types was not detectable. The labeled cells were somewhat enriched in white matter but also present in gray matter with no marked enrichment in any particular brain region. Immunoreactivity was blocked by preincubation with the peptide immunogen (Fig. 5C). The immunoperoxidase label appeared to be perinuclear and extended into the processes (Fig. 5A and B). To identify the IP₃R2-immunoreactive cells, we performed immunofluorescent colocalization experiments (Fig. 6). IP₃R2-immunoreactive cells (Fig. 6C, red fluorescence

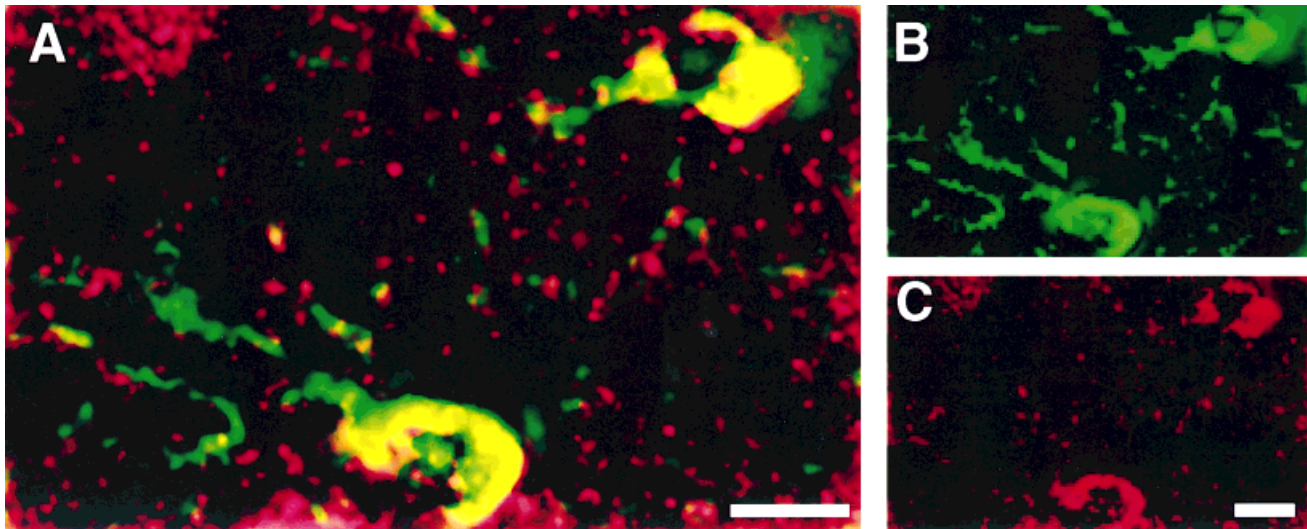


Fig. 6. Immunofluorescent colocalization of inositol 1,4,5-trisphosphate receptors (IP_3R2) to S100- β -immunoreactive astrocytes in rat brain sections. Sections were incubated with monoclonal anti-S100- β and affinity-purified anti- IP_3R2 antibodies (AP42). After washing, S100- β immunoreactivity was detected with fluorescein isothiocyanate (FITC)-labeled anti-mouse secondary antibody (A, green channel)

and IP_3R2 was detected with indocarbocyanine (Cy3)-labeled anti-rabbit secondary (B, same field, red channel). IP_3R2 was present in cells labeled for S100- β , a marker of astrocytes (C, merged images, overlap appears yellow). Omission of either primary antibody gave no signal. Scale bars = 10 μ m.

label) did not colabel with antibodies against glial fibrillary acidic protein (GFAP), a marker of astrocytes (not shown), but did colabel with antibodies against another astrocyte marker, S100- β (Fig. 6B, same field, green label) as indicated by the yellow in the merged images indicating overlap of the two labels (Fig. 6A). The punctate red label not colocalizing with S100- β may be due to a differential distribution of S100- β and IP_3R2 in neuropil of S100- β -positive cells, as IP_3R2 label is generally punctate and S100- β label is weaker in the processes than in the cell soma. Alternatively, IP_3R2 could also be selectively expressed in neuropil of other, unidentified cells. These data indicate that IP_3R2 is present in a population of astrocytes which is GFAP-negative, but S100- β -positive.

Label for IP_3R3 in gray matter was generally suggestive of neuropil. Only faint IP_3R3 label was present in most white matter. In the corpus callosum, for example, this labeling appeared to represent fibers and weakly labeled glial-like cells. Label for IP_3R1 was generally neuronal, consistent with previous reports (Nakanishi et al., 1991; Dent et al., 1996). In white matter, weakly labeled structures appeared to represent only fibers.

Striking differential localizations between the IP_3R1 and the IP_3R3 could be demonstrated in several regions of the brain. For instance, in the bed nucleus of the stria terminalis (BST), the medial portion was enriched in cell bodies labeled for IP_3R1 (Fig. 7A, BSTM), whereas the lateral portion was highly enriched in granular IP_3R3 labeling suggestive of neuropil (Fig. 7D, BSTL). In this area, the labeled neuropil often appeared to surround unlabeled cell bodies (Fig. 9A). In the central nucleus of the amygdala (Ce), the medial portion had cell bodies clearly labeled for IP_3R1 (Fig. 7B, CeM), whereas the lateral portion had IP_3R3 labeling in neuropil, which again often appeared to outline unlabeled cell bodies (Fig. 7E, CeL). The BST and Ce quite closely resembled each other in their patterns of labeling for the distinctly distributed

IP_3R1 and IP_3R3 . These similarities are consistent with similar patterns of labeling for other substances between these two areas noted previously (for example for various neurotransmitters, Martin et al., 1991).

In the cerebellum, Purkinje cells and their dendrites as well as their axons in the white matter were densely labeled for IP_3R1 (Fig. 7C). By contrast, label for IP_3R3 was not enriched in Purkinje cells, but the granule cell layer contained numerous labeled cell bodies and the molecular layer contained a fine granular staining suggestive of a neuropil distribution (Fig. 7F).

In many areas, the neuropil was lightly labeled for IP_3R3 but punctuated by relatively sparsely distributed, intensely labeled structures which appeared to be beaded axons. Examples of this pattern of staining are illustrated for the cortex (Fig. 8A) and caudal spinal trigeminal nucleus (Fig. 8B, for example see asterisk). In the caudal spinal trigeminal nucleus, a deeper layer also contained many labeled fibers with intense punctate staining (Fig. 8B), probably axonal varicosities.

In most regions of the brain, labeling for IP_3R1 appeared to have a predominantly somatic and dendritic appearance, whereas labeling for IP_3R3 was granular or punctate, consistent with labeling of fibers and neuronal terminals, sometimes with a distribution suggestive of perisomatic and peridendritic terminals (for example, Fig. 9A). To determine more precisely the nature of the structures intensely labeled by anti- IP_3R3 , we performed immunoelectron microscopy. Because darkly labeled structures were densely clustered in the laterodorsal division of the BST (BSTLD) as seen in light level views (low magnification in Fig. 7 and higher magnification in Fig. 9A), electron microscopic studies focused on this area (Fig. 9B–D). In low magnification electron micrographs, many intensely labeled structures abutted neuronal somata and dendrites (Fig. 9B). Higher magnification (Fig. 9C) showed that the label was present in synaptic terminals characterized by

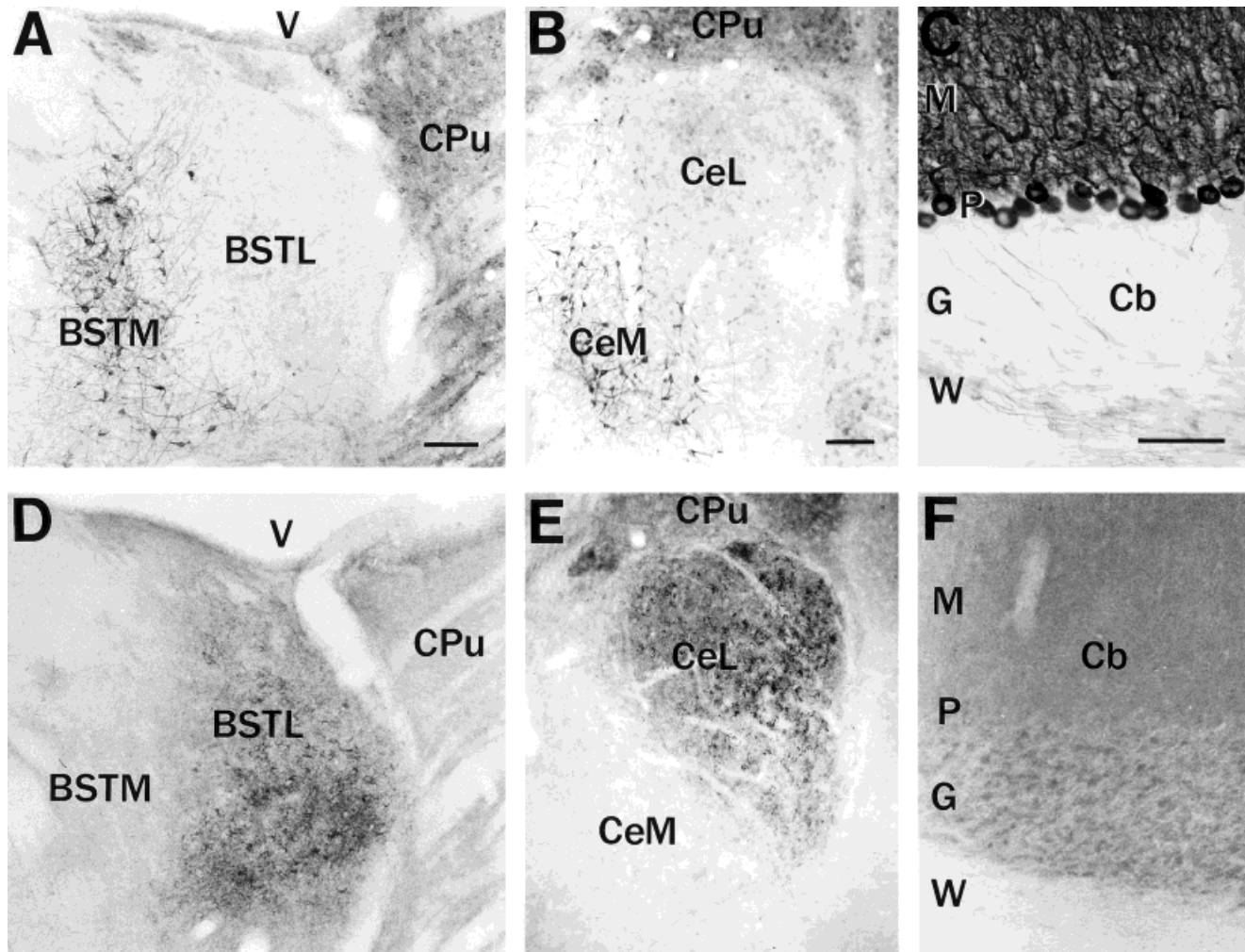


Fig. 7. Distribution of IP₃R1 and IP₃R3 in various regions of rat brain. Nearly adjacent sagittal (A and D, C and F) and coronal (B and E) rat brain sections were stained by an immunoperoxidase method with antibodies against IP₃R1 (Top panels, A, B, C) or IP₃R3 (Bottom panels, D, E, F). IP₃R1 was expressed predominantly in cell bodies and dendrites in the medial portions of the bed nucleus of the stria terminalis (BSTM) (A) and central nucleus of the amygdala (CeM) (B), whereas IP₃R3 was expressed predominantly in neuropil in the lateral

portions of these structures (D, BSTL and E, CeL). In the cerebellar cortex (Cb), IP₃R1 (C) was expressed prominently in Purkinje cell bodies in the Purkinje cell layer (P), dendrites in the molecular layer (M), and axons in the granule cell (G) and white matter (W) layers whereas IP₃R3 (F) was expressed in granule cells and in apparent neuropil in the molecular layer (M). CPu, caudate putamen; V, lateral ventricle. Scale bar = 100 μ m.

prominent presynaptic densities. The most distinctive of these were the large axosomatic terminals that were apparent even at the light microscopic level (Fig. 9A). In the neuropil, the labeled fibers and terminals were small (Fig. 9B). The terminals exhibited round synaptic vesicles, obvious presynaptic densities, and presumably arose from the labeled axons. Control sections which were incubated with antibody preblocked with the peptide antigen, showed no staining. In the control tissue (unobscured by label), the large axosomatic terminals could be seen to contain dense core vesicles, whereas small terminals in the neuropil having distinctive presynaptic densities do not. These data imply that large and small labeled terminals arise from different neuronal sources. Sections processed for optimal morphology (Fig. 9D) also showed that the large pericellular terminals in the BSTLD, structurally identical to the immunolabeled endings, were characterized by the pres-

ence of large dense core vesicles. It is not possible by this method to precisely determine on what membrane the IP₃R3 resides in these terminals. These data show that IP₃R3 is present within some neuronal terminals in the brain, some of which are characterized by the presence of large dense core vesicles.

DISCUSSION

In this study, we have described the differential expression of IP₃R isoforms in the brain. Several considerations indicate that our antibodies specifically recognize the different isoforms. The individual antibodies each yielded single bands on Western blots and the bands for the different isoforms had slightly different migrations in the gels (Fig. 1). Immunoreactivity was abolished by preincubation of the antibodies with the appropriate peptide

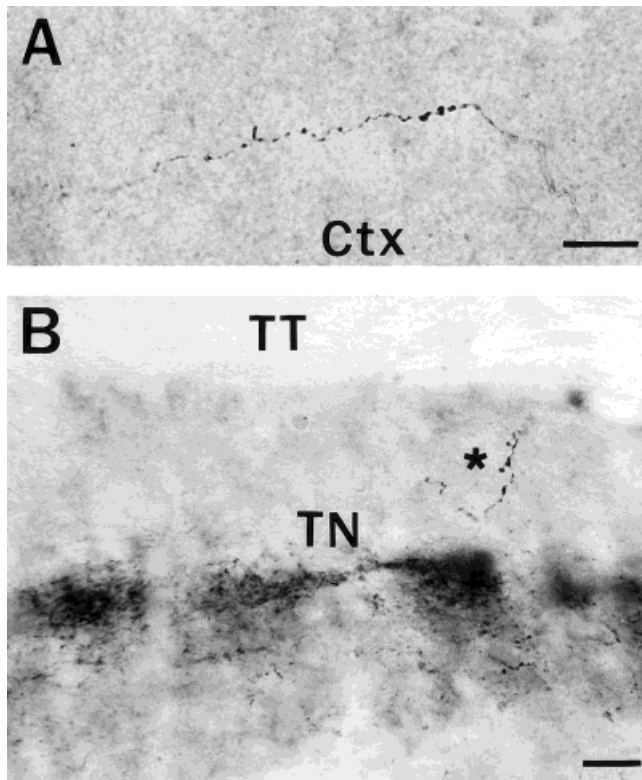


Fig. 8. Expression of IP₃R3 in the rat cerebral cortex (Ctx) and caudal spinal trigeminal nucleus (TN). Intense immunoperoxidase label for IP₃R3 occurred in structures resembling beaded axons scattered through the cortex (A, Ctx) and other parts of the brain including the caudal spinal trigeminal nucleus (B, TN, see asterisk). The trigeminal tract (TT) did not label. In a deeper layer of the TN many labeled fibers displayed intense punctate label along their lengths. Scale bar = 20 μ m.

immunogens. The distributions of IP₃R1 and IP₃R3 in the brain by Western blot analysis differed (Fig. 2A) consistently with the differences detected by immunohistochemistry (Fig. 3). The immunohistochemical label was blocked by preincubation with the appropriate peptides (Figs. 3C and D; 5C), but not by peptides corresponding to the other isoforms. These data demonstrate the specificity of the antibodies used in this report.

Our results, showing the presence and distribution of isoforms other than IP₃R1, are consistent with those of Matsumoto et al. (1996) demonstrating that residual [³H]IP₃ binding, in animals with disruption of IP₃R1 gene, was widespread in the brain. However, in contrast to the primarily neuronal localization of IP₃R3 we observe, Yamamoto-Hino et al. (1995) reported IP₃R3 expression only in astrocytes, ependymal cells, and Bergmann glia in rat brain. In our preparations, labeling of glia for IP₃R3 was virtually absent in comparison to the moderate to dense labeling of neuronal structures. However, the previous study used an antibody raised against a peptide corresponding to human IP₃R3 which differs from the rat sequence. Moreover, the authors introduced another significant alteration, substituting a serine for an internal cysteine to facilitate coupling to carriers via another added cysteine at the N-terminus of the peptide (Sugiyama et al., 1994a). Thus, the antibody may not have appropriate specificity in

rat. In addition, we find that the most intensely IP₃R3-immunoreactive terminals are concentrated in relatively small, discrete regions of the brain that might conceivably be overlooked, especially in the presence of a glial background. Our immunohistochemical localizations of IP₃R3 agree well with the distribution of IP₃R3 in the brain by Western blot analysis, suggesting that the same epitopes are recognized in each method. This comparison was not made by Yamamoto-Hino et al. (1995). Moreover, the anti-IP₃R3 antibody, AP75, selectively labeled cells transfected with the IP₃R3 cDNA and prepared with the same fixative used for immunohistochemistry in the brain (Fig. 4), showing that the antibody can recognize IP₃R3 under these conditions.

The ontogeny of IP₃R1 and IP₃R3 differs, with relatively high expression of IP₃R3 during embryonic development, whereas IP₃R1, consistent with previous studies (Nakanishi et al., 1991; Dent et al., 1996), is expressed highly only postnatally (Fig. 2). What role IP₃R3 might play in development is not yet clear. However, studies in lymphocytes (Khan et al., 1996) have suggested a role for IP₃R3 in apoptosis. Extensive programmed cell death is known to occur during development of the brain (Bredesen, 1995). For example, in mice, there is evidence that massive numbers of cells in the developing cortex may be undergoing programmed cell death around E14 (Blaschke et al., 1996), a stage of development roughly comparable to E16 in the rat, when IP₃R3 is clearly detected in the brain. It is conceivable that IP₃R3 could be involved in programmed cell death in the brain during embryonic development.

We find striking differences in cellular expression of the isoforms. IP₃R2 is expressed predominantly in glial cells with negligible levels detected in neurons (Figs. 5 and 6). In accord with these results, IP₃R2 has been detected at relatively high levels in cultured glial cells (Sheppard et al., 1997; Oberdorf et al., 1997). Glial cells in culture express a variety of neurotransmitters and are capable of producing Ca²⁺ waves through IP₃R activation (Verkhratsky and Kettenmann, 1996; Sheppard et al., 1997). In culture and in hippocampal slices, these Ca²⁺ waves are propagated through glial networks via gap junctions and this process may serve to transmit long-distance signals in the brain (Dani et al., 1992; Verkhratsky and Kettenmann, 1996). Our finding that IP₃R2 is the principal isoform expressed in S100- β astrocytes suggests that, at least in these cells, IP₃R2 is critical in the generation and propagation of Ca²⁺ wave signals. Finally, although we detect IP₃R2 primarily in S100- β -positive cells, it is possible that lower levels are also present in other cells but are undetectable with the present anti-IP₃R2 antibody (AP42).

There were also marked differences between the neuronal patterns of expression of IP₃R1 and IP₃R3. For instance, Purkinje cells in the cerebellum and cartwheel cells of the dorsal cochlear nucleus are highly enriched in IP₃R1, but have low or undetectable levels of IP₃R3. Moreover, granule cells of the cerebellum and many regions of the medulla display moderately high levels of IP₃R3, but IP₃R1 is virtually undetectable in these regions (Figs. 3 and 7).

The intracellular distributions of IP₃R1 and IP₃R3 also vary. There is precedent for IP₃Rs within multiple subcellular compartments (Sharp et al., 1992, 1993a; Bush et al., 1994) as well as for differential distribution of IP₃R and other molecules involved in calcium function in the ER (Otsu et al., 1990; Walton et al., 1991; Takei et al., 1992;

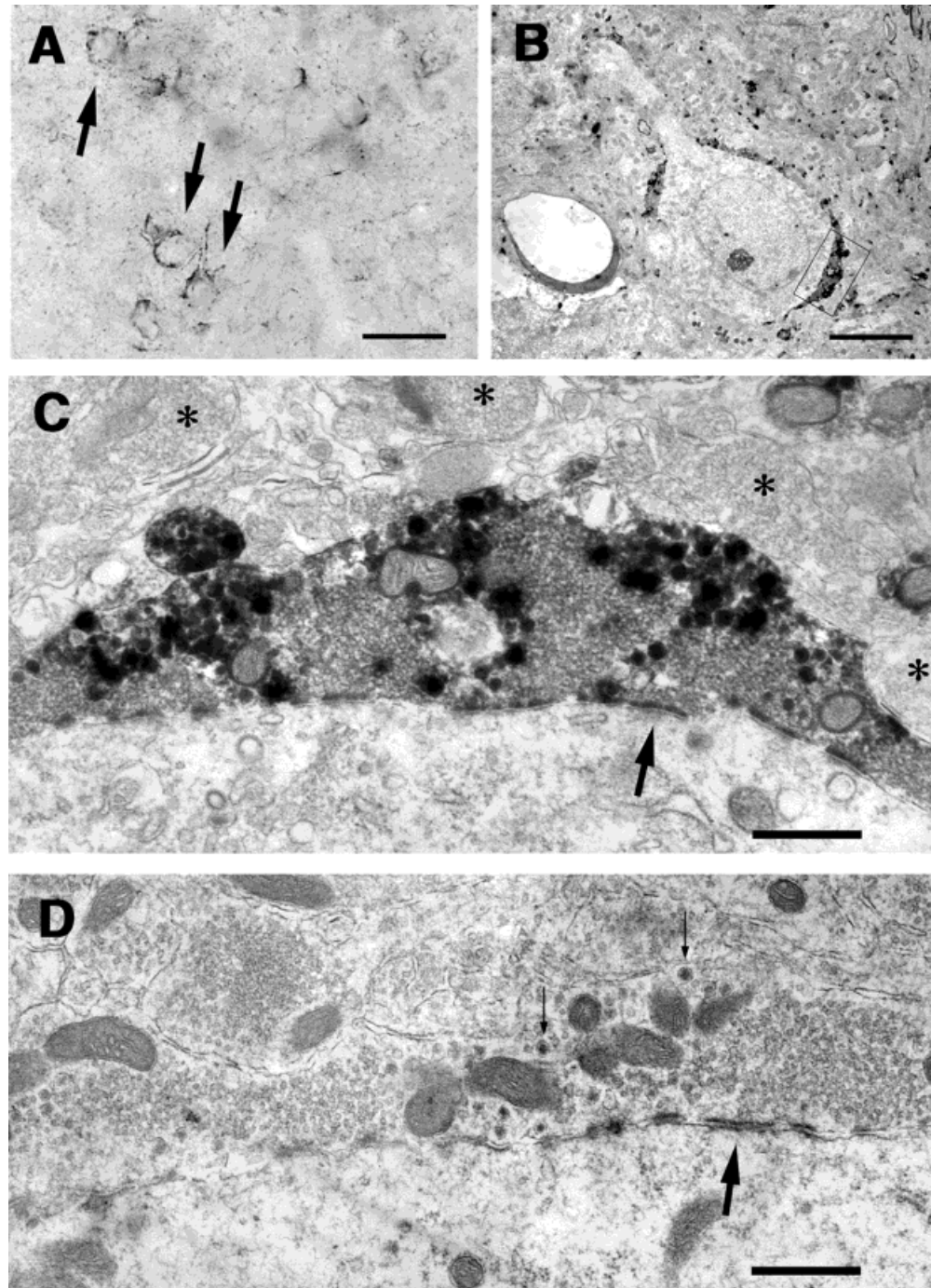


Fig. 9. Localization of inositol 1,4,5-trisphosphate receptors (IP₃R)3 to neuronal terminals. Strongly labeled structures, often adjacent to unlabeled somata and dendrites, were characteristic of the laterodorsal division of the bed nucleus of the stria terminalis (light microscopic view, **A**, arrows; low power electron microscopic view, **B**). **C**: A higher power view of the area boxed in **B** showed that these labeled structures are large neuronal terminals with prominent pre- and postsynaptic densities (arrow) and many small round vesicles. Unlabeled endings are indicated by asterisks. Similar sections, fixed for optimal morphology (4% paraformaldehyde, 2% acrolein) showed that many of the pericellular terminals in this area contain large dense core vesicles (**D**, thin arrows) that are obscured in the labeled endings by the immunoperoxidase reaction product. Thick arrow indicates prominent synaptic density. Control sections, treated with antigen-preadsorbed antibody were blank. Scale bars = 20 μ m in **A**; 5 μ m in **B**; and 0.5 μ m in **C** and **D**.

Villa et al., 1992). IP₃R_s have previously been localized to terminals in retinal neurons by using an antibody which does not distinguish among the different isoforms (Peng et al., 1991). In the brain, IP₃R₁ occurs in terminals in restricted locations, including deep cerebellar nuclei (Mignery et al., 1989; Sharp et al., 1993a, b; Ryugo et al., 1995) and the substantia nigra, pars reticulata (SNR; Worley et al., 1989; and present study). In most regions, IP₃R₁ is predominantly localized in perikarya and dendrites. By contrast, IP₃R₃ is enriched in neuropil and in some regions is clearly present in terminals. For instance, in the BST

and Ce, IP₃R₁ occurs in cell bodies and proximal dendrites, whereas IP₃R₃ is expressed primarily in perisomatic and peridendritic neuronal terminals (Figs. 7 and 9). In many other regions, besides moderate expression in fine neuropil, there is prominent IP₃R₃ expression in scattered structures resembling beaded axons (for example, Fig. 8).

The immunoperoxidase methods using DAB in the present study are not of sufficient resolution to determine the compartment(s) expressing IP₃R₃ within neuronal terminals. To address this question will require more extensive studies using immunogold localization techniques. In other

tissues, besides endoplasmic reticulum, there is some evidence for the presence of IP₃Rs in plasma membrane and transmitter vesicles (Furuichi and Mikoshiba, 1995; Petersen, 1996) although these localizations are controversial (for example, see Nucifora et al., 1996; Yule et al., 1997).

In the BST, the large axosomatic terminals that are immunoreactive for IP₃R3 also frequently contain dense core vesicles, suggesting that they may be peptidergic (Fig. 9D). The appearance of IP₃R3-immunoreactive structures in the Ce is strikingly similar to those in the BST. There is a dense innervation of both the lateral Ce and the lateral division of the BST by peptide-containing terminals, with peptides including somatostatin, neurotensin, and leu-enkephalin (Gray et al., 1982; Martin et al., 1991; Arluison et al., 1994). The BST and Ce are recognized by many as parts of a single continuous structure in the mammalian telencephalon (for example, Martin et al., 1991). Precise roles for nerve terminal IP₃R3 are unclear. Release of intracellular calcium is believed to regulate secretion in endocrine cells (Kasai and Petersen, 1994), and may have a similar role in neurons as well. IP₃R3 might modulate transmitter release or neuronal plasticity in response to presynaptic receptors, such as neuropeptide receptors and certain isoforms of metabotropic glutamate receptors which activate phosphoinositide turnover (Sladeczek et al., 1985; Herrero et al., 1992; Ueda et al., 1996). A role for the phosphoinositide system in synaptic vesicle recycling has been suggested by the discovery of synaptojanin, a presynaptic inositol-5-phosphatase (De Camilli et al., 1996; McPherson et al., 1996). A role for IP₃R has been shown in the regulation of nuclear vesicle fusion during formation of the nuclear membrane in *Xenopus* eggs (Sullivan et al., 1993) raising the possibility that IP₃ receptors might also regulate other membrane fusion events. Obviously, IP₃ receptors play widespread and variable roles in the development and function of the central nervous system, and much more research is needed to clarify these issues.

Because all of our antibodies were raised in rabbits, we have not been able to perform double-label experiments to definitively determine whether differing IP₃R isoforms colocalize in some structures. In some regions, for example, deep cerebellar nuclei and SNR, it is possible that IP₃R1 and IP₃R3 colocalize to the same structures, i.e., neuronal terminals in these regions. In deep cerebellar nuclei, IP₃R3 is only weakly detectable, whereas IP₃R1 label is strong and qualitatively appears somewhat different from the IP₃R3 label. In the SNR, IP₃R3 is present at low levels in smooth neuropil, possibly terminals (Fig. 3). IP₃R1 is strongly expressed in similar structures. However, whereas IP₃R1 is also strongly expressed in descending striatonigral fibers, IP₃R3 is completely undetectable in these fibers. Thus, it seems plausible that IP₃R1- and IP₃R3-stained structures may be distinct in the SNR. Moreover, in this region, prominent IP₃R3 staining is present in scattered, beaded terminal-like structures (similar to those in Fig. 8), which have undetectable IP₃R1 levels (not shown).

A lack of colocalization, at least in most regions, suggests that mixing of IP₃R isoform subunits to form heterotetramers may not occur so extensively in the brain as previously observed in cultured cells (Joseph et al., 1995; Monkawa et al., 1995; Wojcikiewicz and He, 1995; Nucifora et al., 1996). Interestingly, in tissues, IP₃R heterotetramers have only been demonstrated in liver (Monkawa et al., 1995). The

extent to which K⁺ channel subunits form heterotetramers in vivo has also been questioned (Mi et al., 1995). In the case of IP₃Rs, lack of colocalization could be explained by selective expression in differing cells or by targeting to differing subcellular compartments in the same cells. More studies will be required to fully address these questions, including double label experiments, immunoprecipitations, and possibly colchicine injections to help identify the cells expressing IP₃R3. We have previously attempted in situ hybridization to localize IP₃R2 and IP₃R3 mRNAs in the brain without success, presumably because of their relatively low levels in the brain.

Variations in regional localizations of types 1 and 3 IP₃ receptors may reflect different roles in control of behavior. IP₃R3 is most highly expressed in several basal forebrain and limbic system-associated regions including olfactory tubercle, bed nucleus of the stria terminalis, and central nucleus of the amygdala (Figs. 3, 7, and 9). These regions are involved in endocrine, motivational, and autonomic regulation, and receive dopamine and peptide afferents which may be important in regulation of mood (Hilton and Zbrozyna, 1963; Cottle and Calaresu, 1975; Hokfelt et al., 1977; Beckstead et al., 1979; Aggleton and Passingham, 1981; Price and Amaral, 1981; Martin et al., 1991; Aggleton, 1993). The effectiveness of lithium in bipolar affective disorder may relate to actions on the phosphoinositide cycle (Atack et al., 1995; Manji et al., 1995; Warsh and Li, 1996). Accordingly, type 3 IP₃R may be involved in therapeutic effects of lithium on IP₃ turnover in limbic regions.

ACKNOWLEDGMENTS

We thank Tan Pongstaporn for assistance with electron microscopy, and Gabrielle Schilling and Shi-Hua Li for samples from developing rat brain, Lee Martin and Mark Molliver for many helpful discussions, and Audrey McMullan and Mary Cannon for help with immunohistochemistry. We also thank Debbie Pollard for expert manuscript preparation. Solomon H. Snyder supported by USSPHS grant MH18501 and Research Scientist Award DA-00074. Carol Sheppard supported by a grant from National Research Council.

LITERATURE CITED

- Aggleton JP. 1993. The contribution of the amygdala to normal and abnormal emotional states. *Trends Neurosci* 16:328-333.
- Aggleton JP, Passingham RE. 1981. Syndrome produced by lesions of the amygdala in monkeys (*Macaca Mulatta*). *J Comp Physiol Psychol* 95:961-977.
- Arluison M, Brochier G, Vankova M, Leviev V, Villalobos J, Tramou G. 1994. Demonstration of peptidergic afferents to the bed nucleus of the stria terminalis using local injections of colchicine. A combined immunohistochemical and retrograde tracing study. *Brain Res Bull* 34:319-337.
- Atack JR, Broughton HB, Pollack SJ. 1995. Inositol monophosphatase—a putative target for Li⁺ in the treatment of bipolar disorder. *Trends Neurosci* 18:343-349.
- Beckstead RM, Domesick VB, Nauta WJH. 1979. Efferent connections of the substantia nigra and ventral tegmental area in the rat. *Brain Res* 175:191-217.
- Berridge MJ. 1993. Inositol trisphosphate and calcium signalling. *Nature* 361:315-325.
- Bezprozvanny I, Watras J, Ehrlich BE. 1991. Bell-shaped calcium-response curves of Ins(1,4,5)P₃- and calcium-gated channels from endoplasmic reticulum of cerebellum. *Nature* 351:751-754.
- Blaschke AJ, Staley K, Chun J. 1996. Widespread programmed cell death in proliferative and postmitotic regions of the fetal cerebral cortex. *Development* 122:1165-1174.

- Blondel O, Takeda J, Janssen H, Seino S, Bell GI. 1993. Sequence and functional characterization of a third inositol trisphosphate receptor subtype, IP₃R-3, expressed in pancreatic islets, kidney, gastrointestinal tract, and other tissues. *J Biol Chem* 268:11356–11363.
- Bootman MD, Berridge MJ. 1995. The elemental principles of calcium signaling. *Cell* 83:675–678.
- Bredesen DE. 1995. Neural apoptosis. *Ann Neurol* 38:839–851.
- Bush KT, Stuart RO, Li S-H, Moura LA, Sharp AH, Ross CA, Nigam SK. 1994. Epithelial inositol 1,4,5-trisphosphate receptors. Multiplicity of localization, solubility and isoforms. *J Biol Chem* 269:23694–23699.
- Cameron AM, Steiner JP, Sabatini DM, Kaplin AI, Walensky LD, Snyder SH. 1995. Immunophilin FK506 binding protein associated with inositol 1,4,5-trisphosphate receptor modulates calcium flux. *Proc Natl Acad Sci USA* 92:1784–1788.
- Carrington WA, Fogarty KE, Fay FS. 1992. Three-dimensional imaging of single cells using image restoration. In: Foster K, editor. *Noninvasive techniques in cell biology*. New York: Wiley-Liss. p 53–72.
- Carter KC, Bowman D, Carrington W, Fogarty K, McNeil JA, Fay FS, Lawrence JB. 1993. A three-dimensional view of precursor messenger RNA metabolism within the mammalian nucleus. *Science* 259:1330–1335.
- Clapham DE. 1995. Calcium signaling. *Cell* 80:259–268.
- Cottle MKW, Calaresu FR. 1975. Projections from the nucleus tractus solitarius in the cat. *J Comp Neurol* 161:143–158.
- Dani JW, Chernjavsky A, Smith SJ. 1992. Neuronal activity triggers calcium waves in hippocampal astrocyte networks. *Neuron* 8:429–440.
- Danoff SK, Ferris CD, Donath C, Fischer GA, Munemitsu S, Ullrich A, Snyder SH, Ross CA. 1991. Inositol 1,4,5-trisphosphate receptors: Distinct neuronal and nonneuronal forms derived by alternate splicing differ in phosphorylation. *Proc Natl Acad Sci USA* 88:2951–2955.
- De Camilli P, Emr SD, McPherson PS, Novick P. 1996. Phosphoinositides as regulators in membrane traffic. *Science* 271:1533–1539.
- DeLisle S, Blondel O, Longo FJ, Schnabel WE, Bell GI, Welsh MJ. 1996. Expression of inositol 1,4,5-trisphosphate receptors changes the Ca²⁺ signal *Xenopus* oocytes. *Am J Physiol* 270:C1255–C1261.
- Dent MAR, Raisman G, Lai A. 1996. Expression of type 1 inositol 1,4,5-trisphosphate receptor during axogenesis and synaptic contact in the central and peripheral nervous system of developing rat. *Development* 122:1029–1039.
- De Smedt H, Missiaen L, Parys JB, Bootman MD, Mertens L, Van Den Bosch L, Casteels R. 1994. Determination of relative amounts of inositol trisphosphate receptor mRNA isoforms by ratio polymerase chain reaction. *J Biol Chem* 269:21691–21698.
- De Smedt H, Missiaen L, Parys JB, Henning RH, Sienaert I, Vanlingen S, Gijsens A, Himpens B, Casteels R. 1997. Isoform diversity of inositol trisphosphate receptor in cell types of mouse origin. *Biochem J* 322:575–583.
- Ferris CD, Snyder SH. 1992. Inositol 1,4,5-trisphosphate-activated calcium channels. *Ann Rev Physiol* 54:469–488.
- Ferris CD, Haganir RL, Snyder SH. 1990. Calcium flux mediated by purified inositol 1,4,5-trisphosphate receptor in reconstituted lipid vesicles is allosterically regulated by adenine nucleotides. *Proc Natl Acad Sci USA* 87:2147–2151.
- Ferris CD, Haganir RL, Bredt DS, Cameron AM, Snyder SH. 1991. Inositol trisphosphate receptor: Phosphorylation by protein kinase C and calcium-calmodulin dependent protein kinases in reconstituted lipid vesicles. *Proc Natl Acad Sci USA* 88:2232–2235.
- Finch EA, Turner TJ, Goldin SM. 1991. Calcium as a coagonist of inositol 1,4,5-trisphosphate-induced calcium release. *Science* 252:443–446.
- Furuichi T, Mikoshiba K. 1995. Inositol 1,4,5-trisphosphate receptor-mediated Ca²⁺ signaling in the brain. *J Neurochem* 64:953–960.
- Furuichi T, Yoshikawa S, Miyawaki A, Wada K, Maeda N, Mikoshiba K. 1989. Primary structure and functional expression of the inositol 1,4,5-trisphosphate-binding protein P₄₀₀. *Nature* 342:32–38.
- Furuichi T, Simon-Chazottes D, Fujino I, Yamada N, Hasegawa M, Miyawaki A, Yoshikawa S, Guenet J-L, Mikoshiba K. 1993. Widespread expression of inositol 1,4,5-trisphosphate receptor type I gene (*Insp3r1*) in the mouse central nervous system. *Recept Channels* 1:11–24.
- Furuichi T, Kohda K, Miyawaki A, Mikoshiba K. 1994. Intracellular channels. *Curr Opin Neurobiol* 4:294–303.
- Gray TS, Cassell MD, Williams TH. 1982. Synaptology in three peptidergic neuron types in the central nucleus of the rat amygdala. *Peptides* 3:273–281.
- Herrero I, Miras-Portugal MT, Sanchez-Prieto J. 1992. Positive feedback of glutamate exocytosis by metabotropic presynaptic receptor stimulation. *Nature* 360:163–166.
- Hilton SM, Brozyna AW. 1963. Amygdaloid region for defense reactions and its efferent pathway to the brain stem. *J Physiol* 165:160–173.
- Hokfelt T, Johansson O, Fuxe K, Goldstein M, Park D. 1977. Immunohistochemical studies on the localization and distribution of monoamine neuron systems in the rat brain II. Tyrosine hydroxylase in the telencephalon. *Med Biol* 55:21–40.
- Iino M, Endo M. 1992. Calcium-dependent immediate feed-back control of inositol 1,4,5-trisphosphate-induced Ca²⁺ release. *Nature* 360:76–78.
- Joseph SK, Lin C, Pierson S, Thomas AP, Maranto AR. 1995. Heterologomers of type-I and type-III inositol trisphosphate receptors in WB rat liver epithelial cells. *J Biol Chem* 270:23310–23316.
- Kasai H, Peterson OH. 1994. Spatial dynamics of second messengers: IP₃ and cAMP as long-range and associative messengers. *Trends Neurosci* 17:95–101.
- Khan AA, Steiner JP, Klein MG, Schneider MF, Snyder SH. 1992. IP₃ receptor: Localization to plasma membrane and co-capping with the T cell receptor. *Science* 257:815–818.
- Khan AA, Soloski MJ, Sharp AH, Schilling G, Sabatini DM, Li S-H, Ross CA, Snyder SH. 1996. Lymphocyte apoptosis: Mediated by increased type 3 inositol 1,4,5-trisphosphate receptor. *Science* 273:503–507.
- Mailleux P, Takazawa K, Erneux C, Vanderhaeghen J-J. 1992. Comparison of neuronal inositol 1,4,5-trisphosphate 3-kinase and receptor mRNA distributions in the adult rat brain using in situ hybridization histochemistry. *Neuroscience* 49:577–590.
- Manji HK, Potter WZ, Lenox RH. 1995. Signal transduction pathways. Molecular targets for lithium's actions. *Arch Gen Psychiat* 52:531–543.
- Maranto AR. 1994. Primary structure, ligand binding, and localization of the human type 3 inositol 1,4,5-trisphosphate receptor expressed in intestinal epithelium. *J Biol Chem* 269:1222–1230.
- Martin LJ, Powers RE, Dellovade TL, Price DL. 1991. The bed nucleus-amygdala continuum in human and monkey. *J Comp Neurol* 309:445–485.
- Matsumoto M, Nakagawa T, Inoue T, Nagata E, Tanaka K, Tankano H, Minowa O, Kuno J, Sakakibara S, Yamada M, Yoneshima H, Miyawaki A, Fukuuchi Y, Furuichi T, Okano H, Mikoshiba K, Noda T. 1996. Ataxia and epileptic seizures in mice lacking type 1 inositol 1,4,5-trisphosphate receptor. *Nature* 379:168–171.
- McCarthy KD, de Vellis J. 1980. Preparation of separate astroglial and oligodendroglial cell cultures from rat cerebral tissue. *J Cell Biol* 85:890–902.
- McPherson PS, Garcia EP, Slepnev VI, David C, Zhang X, Grabs D, Sossin WS, Bauerfeind R, Nemoto Y, De Camilli P. 1996. A presynaptic inositol-5-phosphatase. *Nature* 379:353–357.
- Mi H, Deerinck TJ, Ellisman MH, Schwartz TL. 1995. Differential distribution of closely related potassium channels in rat Schwann cells. *J Neurosci* 15:3761–3774.
- Mignery GA, Südhof TC, Takei K, De Camilli P. 1989. Putative receptor for inositol 1,4,5-trisphosphate similar to ryanodine receptor. *Nature* 342:192–195.
- Mignery GA, Newton CL, Archer BT III, Südhof TC. 1990. Structure and expression of the rat inositol 1,4,5-trisphosphate receptor. *J Biol Chem* 265:12679–12685.
- Monkawa T, Miyawaki A, Sugiyama T, Yoneshima H, Yamamoto-Hino M, Furuichi T, Saruta T, Hasegawa M, Mikoshiba K. 1995. Heterotrimeric complex formation of inositol 1,4,5-trisphosphate receptor subunits. *J Biol Chem* 270:14700–14704.
- Mourey RJ, Supattapone S, Snyder SH. 1989. Purification and characterization of inositol-1,4,5-trisphosphate binding sites in rat peripheral tissue. *Neurosci Abstr* 14:84.
- Nakagawa T, Shiota C, Okano H, Mikoshiba K. 1991. Differential localization of alternative spliced transcripts encoding inositol 1,4,5-trisphosphate receptors in mouse cerebellum and hippocampus: In situ hybridization study. *J Neurochem* 59:1807–1810.
- Nakanishi S, Maeda N, Mikoshiba K. 1991. Immunohistochemical localization of an inositol 1,4,5-trisphosphate receptor, P₄₀₀, in neural tissue: Studies in developing and adult mouse brain. *J Neurosci* 11:2075–2086.
- Newton CL, Mignery GA, Südhof TC. 1994. Co-expression in vertebrate tissues and cell lines of multiple inositol 1,4,5-trisphosphate (InsP₃) receptors with distinct affinities for InsP₃. *J Biol Chem* 269:28613–28619.
- Nucifora FC Jr, Li S-H, Danoff S, Ullrich A, Ross CA. 1995. Molecular cloning of a cDNA for the human inositol 1,4,5-trisphosphate receptor

- type 1, and the identification of a third alternatively spliced variant. *Mol Brain Res* 32:291–296.
- Nucifora FC Jr, Sharp AH, Milgram SL, Ross CA. 1996. Inositol 1,4,5-trisphosphate receptors in endocrine cells: Localization and association in hetero- and homotetramers. *Mol Biol Cell* 7:949–960.
- Oberdorf J, Vallano ML, Wojcikiewicz RJH. 1997. Expression and regulation of types I and II inositol 1,4,5-trisphosphate receptors in rat cerebellar granule cell preparations. *J Neurochem* 69:1897–1903.
- Osborn M, Weber K. 1982. Immunofluorescence and immunocytochemical procedures with affinity purified antibodies: Tubulin-containing structures. *Methods Cell Biol* 24:97–132.
- Otsu H, Yamamoto A, Maeda N, Mikoshiba K, Tashiro Y. 1990. Immunogold localization of inositol 1,4,5-trisphosphate (InsP₃) receptor in mouse cerebellar Purkinje cells using three monoclonal antibodies. *Cell Struct Funct* 15:163–173.
- Parys JB, De Smedt H, Missiaen L, Bootman MD, Sienaert I, Casteels R. 1995. Rat basophilic leukemia cells as model system for inositol 1,4,5-trisphosphate receptor IV, a receptor of the type II family: Functional comparison and immunological detection. *Cell Calcium* 17:239–249.
- Paxinos G, Watson C. 1986. *The rat brain in stereotaxic coordinates*. San Diego, CA: Academic Press.
- Peng Y-W, Sharp AH, Snyder SH, Yau K-W. 1991. Localization of the inositol 1,4,5-trisphosphate receptor in synaptic terminals in the vertebrate retina. *Neuron* 6:525–521.
- Petersen OH. 1996. Can Ca²⁺ be released from secretory granules or synaptic vesicles? *Trends Neurosci* 19:411–413.
- Price JL, Amaral DG. 1981. An autoradiographic study of the projections of the central nucleus of the monkey amygdala. *J Neurosci* 1:1242–1259.
- Ross CA, Meldolesi J, Milner TA, Satoh T, Supattapone S, Snyder SH. 1989. Inositol (1,4,5) trisphosphate receptor localized to endoplasmic reticulum in cerebellar Purkinje neurons. *Nature* 339:468–470.
- Ross CA, Bredt D, Snyder SH. 1990. Messenger molecules in the cerebellum. *Trends Neurosci* 13:216–222.
- Ross CA, Danoff SK, Schell MJ, Snyder SH, Ullrich A. 1992. Three additional inositol 1,4,5-trisphosphate receptors: Molecular cloning and differential localization in brain and peripheral tissues. *Proc Natl Acad Sci USA* 89:4265–4269.
- Ryugo DK, Dodds LW, Benson TE, Kiang NYS. 1991. Unmyelinated axons of the auditory nerve in cats. *J Comp Neurol* 308:209–223.
- Ryugo DK, Pongstaporn T, Wright DD, Sharp AH. 1995. Inositol 1,4,5-trisphosphate receptors: Immunocytochemical localization in the dorsal cochlear nucleus. *J Comp Neurol* 358:102–118.
- Satoh T, Ross CA, Villa A, Supattapone S, Pozzan T, Snyder SH, Meldolesi J. 1990. The inositol 1,4,5-trisphosphate receptor in cerebellar Purkinje cells: Quantitative immunogold labeling reveals concentration in an ER subcompartment. *J Cell Biol* 111:615–624.
- Schell MJ, Danoff SK, Ross CA. 1993. Inositol (1,4,5)-trisphosphate receptor: Characterization of neuron-specific alternative splicing in rat brain and peripheral tissues. *Mol Brain Res* 17:212–216.
- Sharp AH, Snyder SH, Nigam SK. 1992. Inositol 1,4,5-trisphosphate receptors: Localization in epithelial tissue. *J Biol Chem* 267:7444–7449.
- Sharp AH, McPherson PS, Dawson TM, Aoki C, Campbell KP, Snyder SH. 1993a. Differential immunohistochemical localization of inositol 1,4,5-trisphosphate- and ryanodine-sensitive Ca²⁺ release channels in rat brain. *J Neurosci* 13:3051–3063.
- Sharp AH, Dawson TM, Ross CA, Fotuhi M, Mourey RJ, Snyder SH. 1993b. Inositol 1,4,5-trisphosphate receptors: Immunohistochemical localization to discrete areas of rat brain. *Neuroscience* 53:927–942.
- Sheppard CA, Simpson PB, Sharp AH, Nucifora FC, Jr, Ross CA, Lange GD, Russell JT. 1997. Comparison of type 2 inositol 1,4,5-trisphosphate receptor distribution and subcellular Ca²⁺ release sites that support Ca²⁺ waves in cultured astrocytes. *J Neurochem* 68:2317–2327.
- Simpson PB, Challiss RAJ, Nahorski SR. 1995. Neuronal Ca²⁺ stores: Activation and function. *Trends Neurosci* 18:299–306.
- Sladeczek F, Pin J-P, Recasens M, Bockaert J, Weiss S. 1985. Glutamate stimulates inositol phosphate formation in striatal neurons. *Nature* 317:717–719.
- Strigrow F, Ehrlich BE. 1996. Ligand-gated calcium channels inside and out. *Curr Opin Cell Biol* 8:490–495.
- Südhof TC, Newton CL, Archer BT III, Ushkaryov YA, Mignery GA. 1991. Structure of a novel InsP₃ receptor. *EMBO J* 10:3199–3206.
- Sugiyama T, Furuya A, Monkawa T, Yamamoto-Hino M, Satoh S, Ohmori K, Miyawaki A, Hanai N, Mikoshiba K, Hasegawa M. 1994a. Monoclonal antibodies distinctively recognizing the subtypes of inositol 1,4,5-trisphosphate receptor: Application to the studies on inflammatory cells. *FEBS Lett* 354:149–154.
- Sugiyama T, Yamamoto-Hino M, Miyawaki A, Furuichi T, Mikoshiba K, Hasegawa M. 1994b. Subtypes of inositol 1,4,5-trisphosphate receptor in human hematopoietic cell lines: Dynamic aspects of their cell-type specific expression. *FEBS Lett* 349:191–196.
- Sullivan KMC, Busa WB, Wilson KL. 1993. Calcium mobilization is required for nuclear vesicle fusion in vitro: Implications for membrane traffic and IP₃ receptor function. *Cell* 73:1411–1422.
- Supattapone S, Worley PF, Baraban JM, Snyder SH. 1988. Solubilization, purification, and characterization of an inositol trisphosphate receptor. *J Biol Chem* 263:1530–1534.
- Takei K, Stukenbrok H, Metcalf A, Mignery GA, Südhof TC, Volpe P, De Camilli P. 1992. Ca²⁺ stores in Purkinje neurons: Endoplasmic reticulum subcompartments demonstrated by the heterogeneous distribution of the InsP₃ receptor, Ca²⁺-ATPase, and calsequestrin. *J Neurosci* 12:489–505.
- Ueda H, Tamura S, Fukushima N, Katada T, Ui M, Satoh M. 1996. Inositol 1,4,5-trisphosphate-gated calcium transport through plasma membranes in nerve terminals. *J Neurosci* 16:2891–2900.
- Verkhratsky A, Kettenmann H. 1996. Calcium signalling in glial cells. *Trends Neurosci* 19:346–352.
- Villa A, Sharp AH, Racchetti G, Podini P, Bole DG, Dunn WA, Pozzan T, Snyder SH, Meldolesi J. 1992. The endoplasmic reticulum of Purkinje neuron body and dendrites: Molecular identity and specializations for Ca²⁺ transport. *Neuroscience* 49:467–477.
- Walton PD, Airey JA, Sutko JL, Beck CF, Mignery GA, Südhof TC, Deerinck TJ, Ellisman MH. 1991. Ryanodine and inositol trisphosphate receptors coexist in avian cerebellar Purkinje neurons. *J Cell Biol* 113:1145–1157.
- Warsh JJ, Li PP. 1996. Second messenger systems and mood disorders. *Curr Opin Psychiat* 9:23–29.
- Wojcikiewicz RJH. 1995. Type I, II, and III inositol 1,4,5-trisphosphate receptors are unequally susceptible to down-regulation and are expressed in markedly different proportions in different cell types. *J Biol Chem* 270:11678–11683.
- Wojcikiewicz RJH, He Y. 1995. Type I, II and III inositol 1,4,5-trisphosphate receptor co-immunoprecipitation as evidence for the existence of heterotetrameric receptor complexes. *Biochem Biophys Res Comm* 213:334–341.
- Worley PF, Baraban JM, Snyder SH. 1989. Inositol 1,4,5-trisphosphate receptor binding: autoradiographic localization in rat brain. *J Neurosci* 9:338–346.
- Yamamoto-Hino M, Miyawaki A, Kawano H, Sugiyama T, Furuichi T, Hasegawa M, Mikoshiba K. 1995. Immunohistochemical study of inositol 1,4,5-trisphosphate receptor type 3 in rat central nervous system. *NeuroReport* 6:273–276.
- Yule DI, Ernst SA, Hirohide O, Wojcikiewicz RJH. 1997. Evidence that zymogen granules are not a physiologically relevant calcium pool. *J Biol Chem* 272:9093–9098.